CHAPTER IV
RESULTS AND DISCUSSION

4.1 Permeability and Selectivity for Ultem Membrane and Zeolite-Ultem MMMs

The permeability measurement for Ultem membrane and Zeolite-Ultem MMMs with NaX, AgX and silicalite incorporated at various loadings of 10, 20 and 30 wt % were conducted to determine the gas permeability and C_3H_6/C_3H_8 selectivity for each MMM. The same calculation of such properties is provided in Appendix A

The permeabilities of nitrogen, P_{N2}; propane, P_{C3H8}; propylene, P_{C3H6} and the selectivity of propylene to propane, P_{C3H6}/P_{C3H8} presented in Table 4.1 were determined at steady state permeation rates for each gas passing through the membrane at room temperature and pressure difference of 50 psi.

Table 4.1 Permeabilities of gases and Selectivity of C_3H_6/C_3H_8 for Ultem Membrane and Zeolite-Ultem MMMs

Membrane	Permeability (P) (cm^3 (STP).cm/cm^2.s.cmHg)			C_3H_6/C_3H_8 Selectivity
	N_2	C_3H_6	C_3H_8	
Ultem membrane	1.196E-11	6.723E-12	1.462E-12	4.60
10wt% SL-Ultem MMM	1.768E-11	7.278E-12	7.121E-12	1.02
20wt% SL-Ultem MMM	1.857E-11	8.134E-12	8.475E-12	0.96
30wt% SL-Ultem MMM	2.412E-11	1.725E-11	1.419E-11	1.22
10wt%NaX-Ultem MMM	4.608E-11	1.572E-11	3.250E-12	4.84
20wt%NaX-Ultem MMM	7.698E-11	3.875E-11	8.780E-12	4.41
30wt%NaX-Ultem MMM	8.588E-11	3.992E-11	9.116E-12	4.38
10wt%AgX-Ultem MMM	3.010E-11	1.316E-11	4.324E-12	3.04
20wt%AgX-Ultem MMM	3.482E-11	1.424E-11	4.678E-12	3.04
30wt%AgX-Ultem MMM	3.945E-11	1.502E-11	5.013E-12	3.00

The diffusivity term is usually dominant for separation performance in glassy polymer, refer to the permeability falls with increasing molecular size and smaller molecule permeate preferentially (Othmer *et al.*, 1981). Since N_2 is the smallest molecule studies, its permeability for Ultem membrane is the highest. through Ultem membrane. In cases of C_3H_6 and C_3H_8, their molecular sizes are quite similar, therefore the solubility term must be taken into consideration for describing such properties. The solubility of gas in polymer membrane depends on the polymer-penetrant interactions. Because of their higher polarisability and flat configuration due to the presence of the π electrons of olefins, they are more favorable to be sorbed possibly in polymer membrane. This is because, with higher electron density in the olefins, the oscilation of electrons is enhanced. This results in

better interactions between C_3H_6 and Ultem chain segments (Chan *et al.*, 2002). Consequently, the Ultem membrane is selective to C_3H_6 over C_3H_8.

4.1.1 Silicalite-Ultem MMMs

The gas permeabilities and C_3H_6/C_3H_8 selectivity of Silicalite-Ultem MMMs are shown in Figure 4.1.

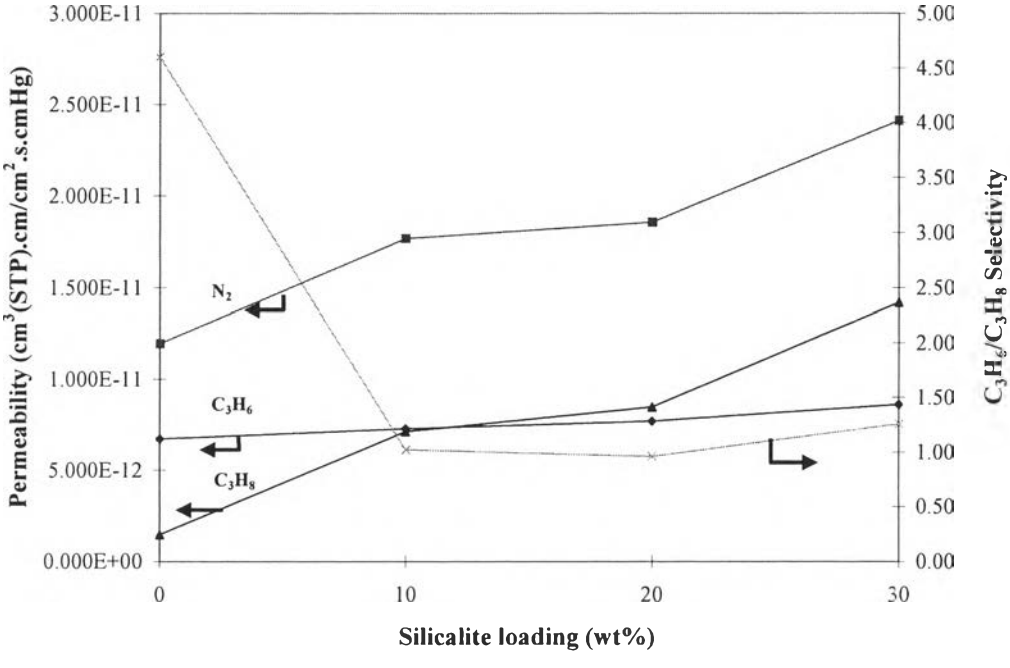

Figure 4.1 Gas permeabilities and C_3H_6/C_3H_8 selectivity of Silicalite-Ultem MMMs.

It is clearly seen from the figure that the incorporation of silicalite into Ultem membrane resulted in increasing the N_2, C_3H_6 and C_3H_8 permeabilities as increasing silicalite loading; however, a decrease in C_3H_6/C_3H_8 selectivity was observed when compared to that of Ultem membrane. Such a decrease was found to be independent of the amount of Silicalite loaded in the membrane matrix. The SEM image of Silicalite-Ultem MMM is shown in Figure 4.2 (a). The micrographs indicated a homogeneous distribution of Silicalite in the polymer matrix. However, there are small

channels or microvoids between zeolite surfaces and polymer phase. It is believed to result from a partial incompatibility between them, implying that the polymer interacted weakly with the zeolite particles (Duval *et al.*, 1994). This appears three phases, instead of two present in MMM: polymer, zeolite, and unexpected nonselective voids around zeolite particles. When nonselective voids occur in the matrix, these voids allow gas to bypass around zeolite particles, leading to the increase in its permeability compared to that for the Ultem membrane. The N_2, C_3H_6 and C_3H_8 permeabilities increase with increasing silicalite content. It is believed that nonselective voids might form continuous pathways when the amount of Silicalite incorporated into polymer matrix increases. This contributes to poor separation performance.

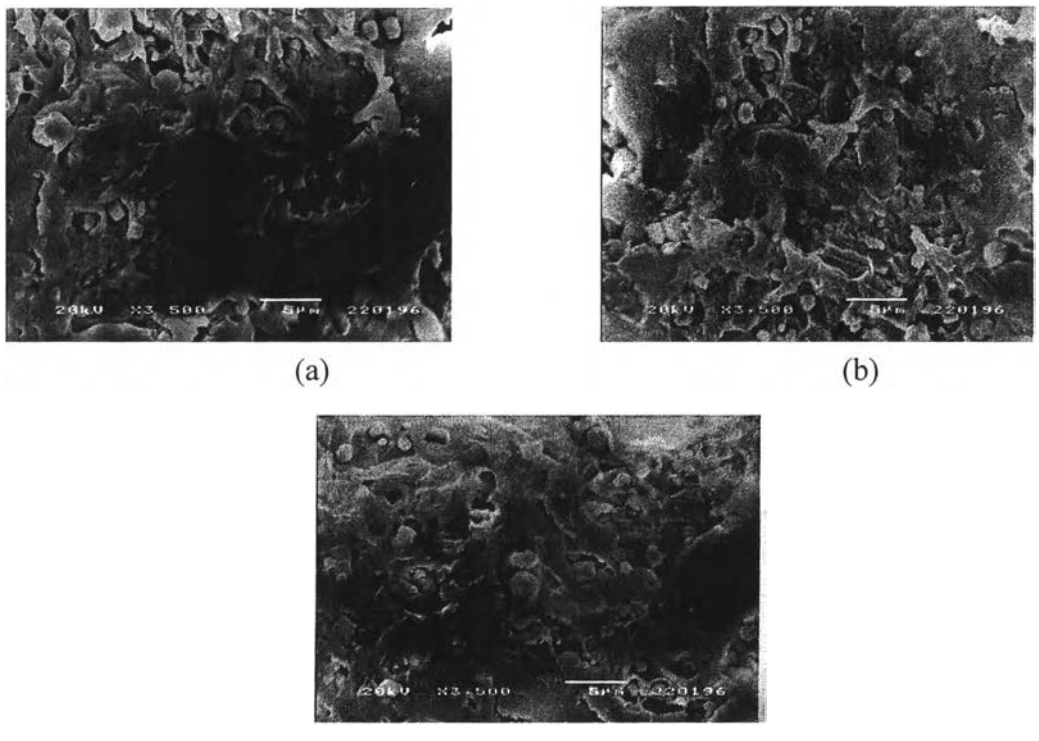

(a) (b)

(c)

Figure 4.2 SEM images showing the morphology of 20 wt% Zeolite-Ultem MMMs; (a) Silicalite-Ultem MMM, (b) Nax-Ultem MMM and (c) AgX-Ultem MMM.

4.1.2 NaX-Ultem MMMs

The permeabilities and C_3H_6/C_3H_8 selectivity of NaX-Ultem MMMs are shown in Figure 4.3.

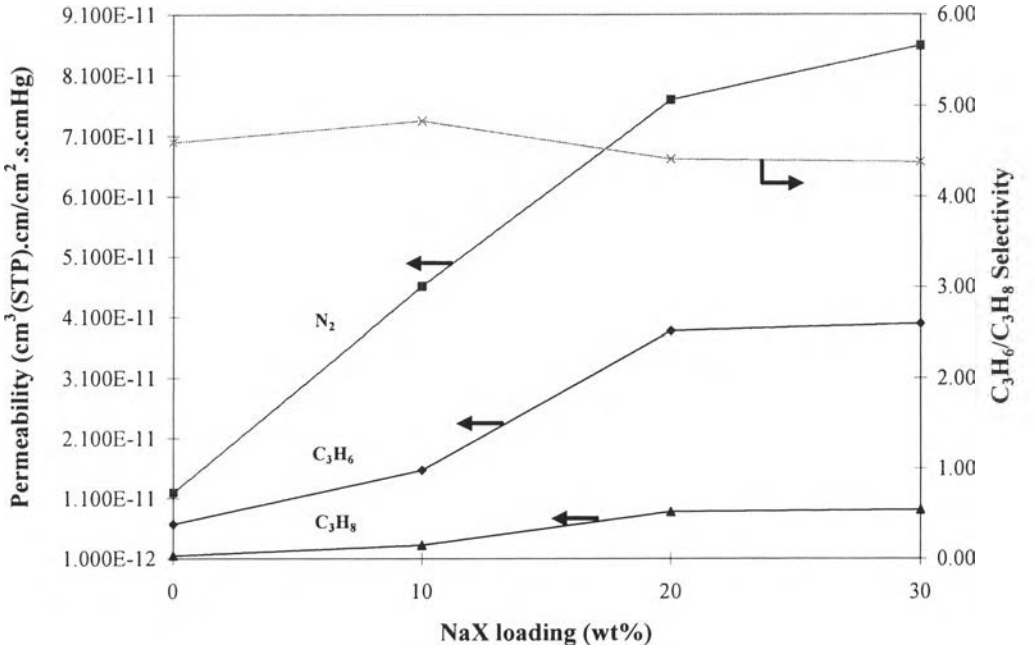

Figure 4.3 Gas permeabilities and C_3H_6/C_3H_8 selectivity of NaX-Ultem MMMs.

Incorporation of NaX into Ultem membrane resulted in increases in the N_2, C_3H_6 and C_3H_8 permeabilities with increasing NaX loading; however, the C_3H_6/C_3H_8 selectivity not change significantly when compared to that of Ultem membrane. It was found to be independent of the amount of NaX loaded in the membrane matrix. The morphology of NaX-Ultem MMM is shown in Figure 4.2 (b). The micrographs indicated a homogeneous distribution of NaX in the polymer matrix. Moreover, the nonselective voids were found in the membrane matrix. The explanation for void formation is postulated as same as that for Slicalite-Ultem MMMs. The N_2, C_3H_6 and C_3H_8 permeabilities increased with increasing NaX loading. Even through voids appear in the matrix, the C_3H_6/C_3H_8 separation probably takes place predominantly in the Ultem polymeric phase, therefore this is the reason for unchanging in $C_3H_6/C3H_8$ selectivities.

4.1.3 AgX-Ultem MMMs

The permeabilities and C_3H_6/C_3H_8 selectivity of AgX-Ultem MMMs are shown in Figure 4.4.

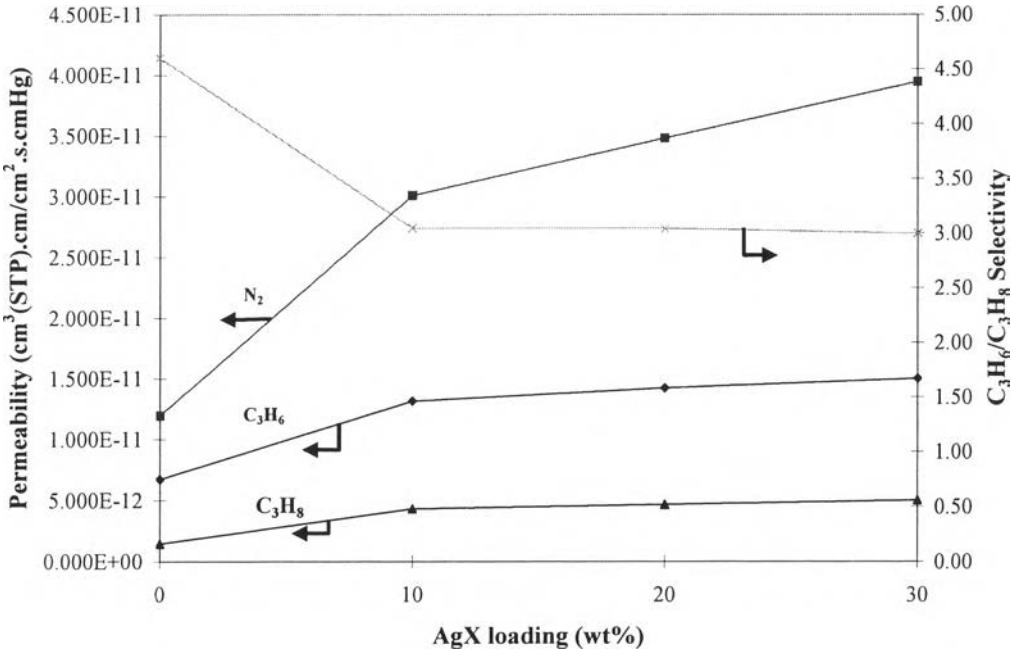

Figure 4.4 The permeabilities and the C_3H_6/C_3H_8 selectivity of AgX-Ultem MMMs.

Incorporation of AgX into Ultem membrane resulted in increase in the N_2, C_3H_6 and C_3H_8 permeabilities with increasing AgX loading; however, the C_3H_6/C_3H_8 selectivity decrease when compared to that of Ultem membrane. It was found to be independent of the amount of AgX loaded in the membrane matrix. A homogeneous distribution of AgX in the membrane matrix and nonselective voids was observed as clearly seen from the morphology of AgX-Ultem MMM in Figure 4.2 (c). The N_2, C_3H_6 and C_3H_8 permeabilities increased with increasing AgX loading. The results obtained could be explained in the same reasons as given for the other types of zeolite.

Obviously, the attempts to fabricating MMMs using glassy polymers and zeolites resulted in the presence of voids at the polymer-zeolite interface, thus reducing the separation performance relatively to that of pure polymer membrane.

Many researchers have identified difficulties with obtaining good polymer-zeolite contact with glassy polymers, such as polyimide. Such glassy polymer mixed matrix membranes often demonstrate poor polymer-zeolite adhesion, resulting in nonselective voids and no selectivity enhancement. It was postulated that because of the high chain rigidity of polyimide, their close packing is disturbed in the vicinity of the zeolite particles, resulting in void formation in the mixed matrix membrane (Mahajan *et al.* 2000).

4.2 Modification of Zeolite Surface

To overcome the problem of void formation in the membrane matrix, An aminopropyltrimethoxy silane agent was systematically investigated to improve adhesion between polymer chains and zeolite particles.

4.2.1 Spectroscopy Results

The IR spectra of zeolite, coupling agent and zeolite with coupling agent are presented in Figure 4.5.

There are four main peaks with the ascending wave numbers showing the characteristics of zeolite ; the vibration mode of zeolite framework to the bending of the TO_4 tetrahedra, to the structure sensitive double five-membered ring vibration, and to symmetric and asymmetric stretching vibration of the T-O-T linkages, respectively.

Silicalite has the main peaks at 450, 550, 800, and 1100 cm^{-1}, respectively. For NaX and AgX, they show the similar four main peaks at 460, 560, 670-750, and 980 cm^{-1}, respectively. Aminopropyltrimethoxy silane (APTS) shows the 1100 cm^{-1} peak typical of the Si-O peak of the Si-O-C group and the sharp C-H peak of the Si-O-CH_3 group at 2840 cm^{-1} The amino group at around 3300 cm^{-1} is only visible at higher scale expansion. In contrast, after mixing the zeolites and APTS, the 1100 cm^{-1} peak of APTS disappeared, as the Si-O-C links are replaced by Si-O-Si bands in which it shows broad adsorption from 1100 to 1000 cm^{-1}. The 2860 and 2930 cm^{-1} peaks visible in the product was attributed to the $-CH_2-$ adsorption of

the amine group. This infered that molecules of the silane coupling agent were grafted onto the external surface of zeolite.

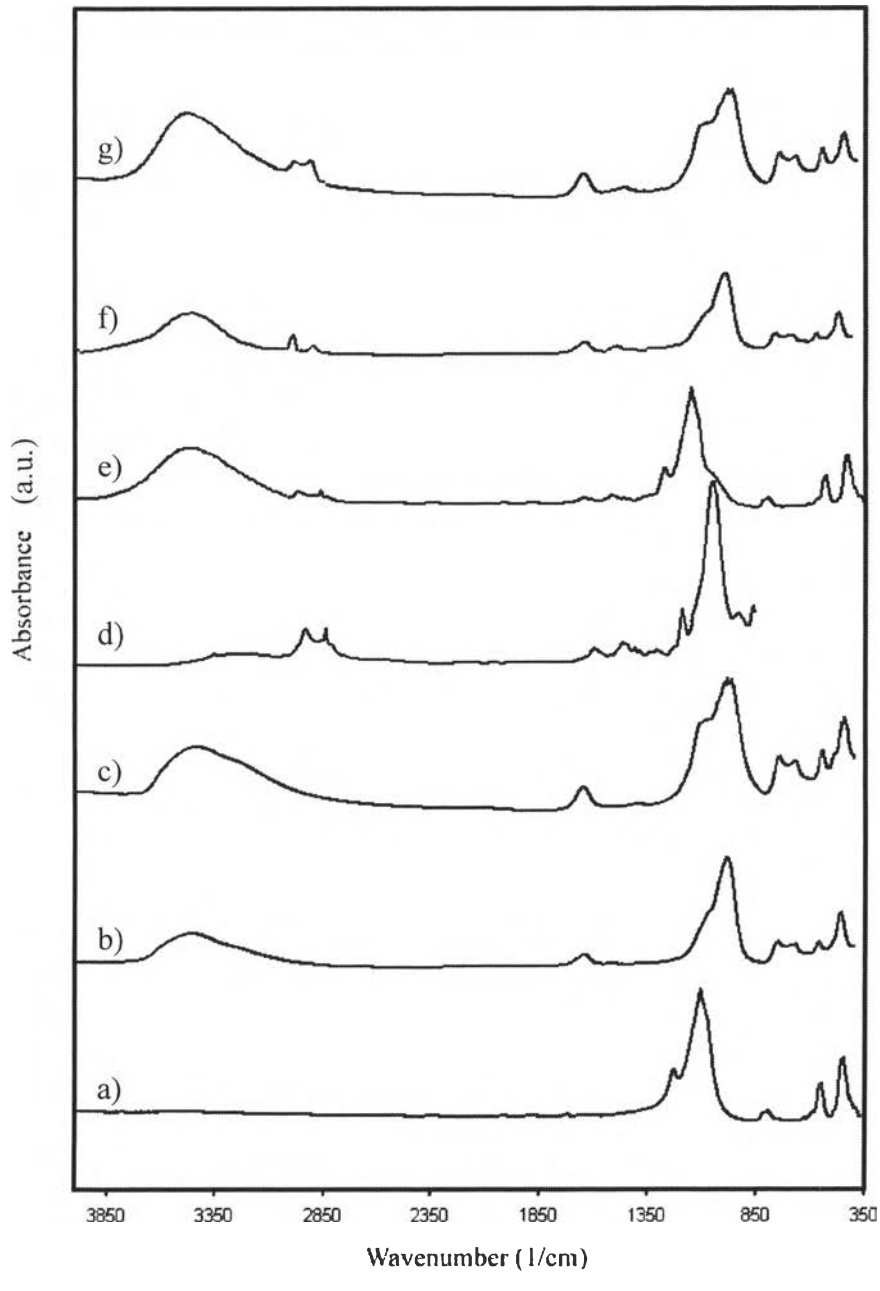

Figure 4.5 FTIR spectra for zeolite; (a) silicalite, (b) NaX and (c) AgX, (d) Aminopropyltrimethoxy silane (APTS) and modified zeolite; (e) modified silicalite , (f) modified NaX and (g) modified AgX.

It is believed that the strongest possible interaction between modified zeolites and Ultem chains was possible to be hydrogen bonding in which a carbonyl

group of polymer reacts with an amino group of the coupling agent (Yong et al. 2001), subsequently binds to the zeolite surface by a reaction of silyl ether with zeolite-OH and polymer chain as schematically shown in Figures 4.6 and 4.7,respectively.

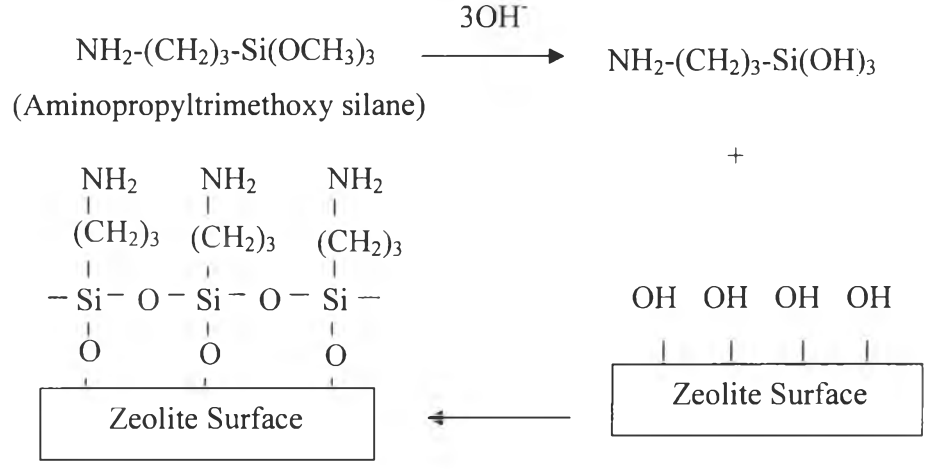

Figure 4.6 Principle of reaction of aminopropyltrimethoxy silane (APTS) onto zeolite surface.

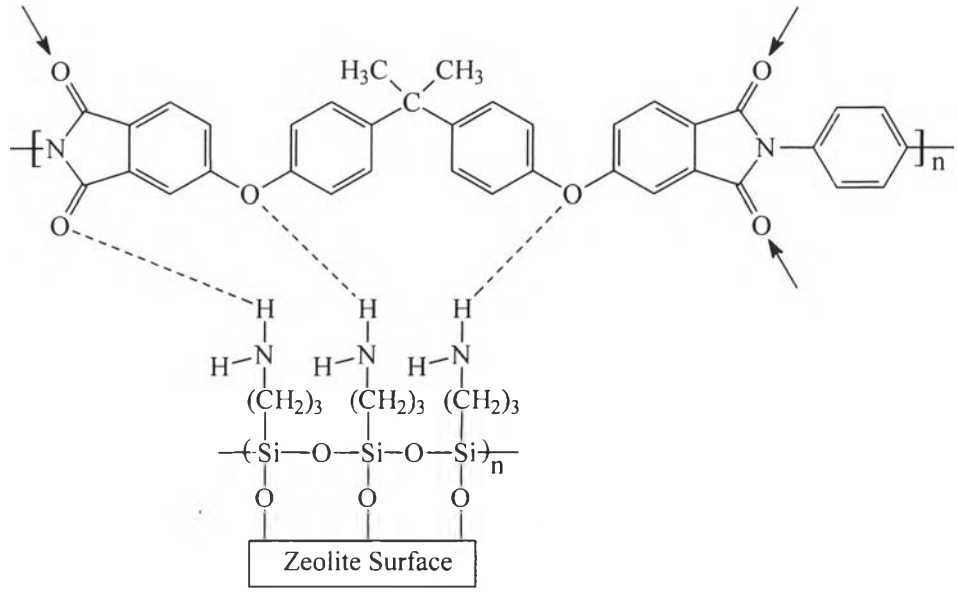

Figure 4.7 Interaction between modified zeolite and Ultem chain polymer.

4.2.2 Microscopy Results

Figure 4.3 shows the SEM images of the cross-sectional morphology of Ultem filled with modified Silicalite, NaX and AgX zeolite MMMs.

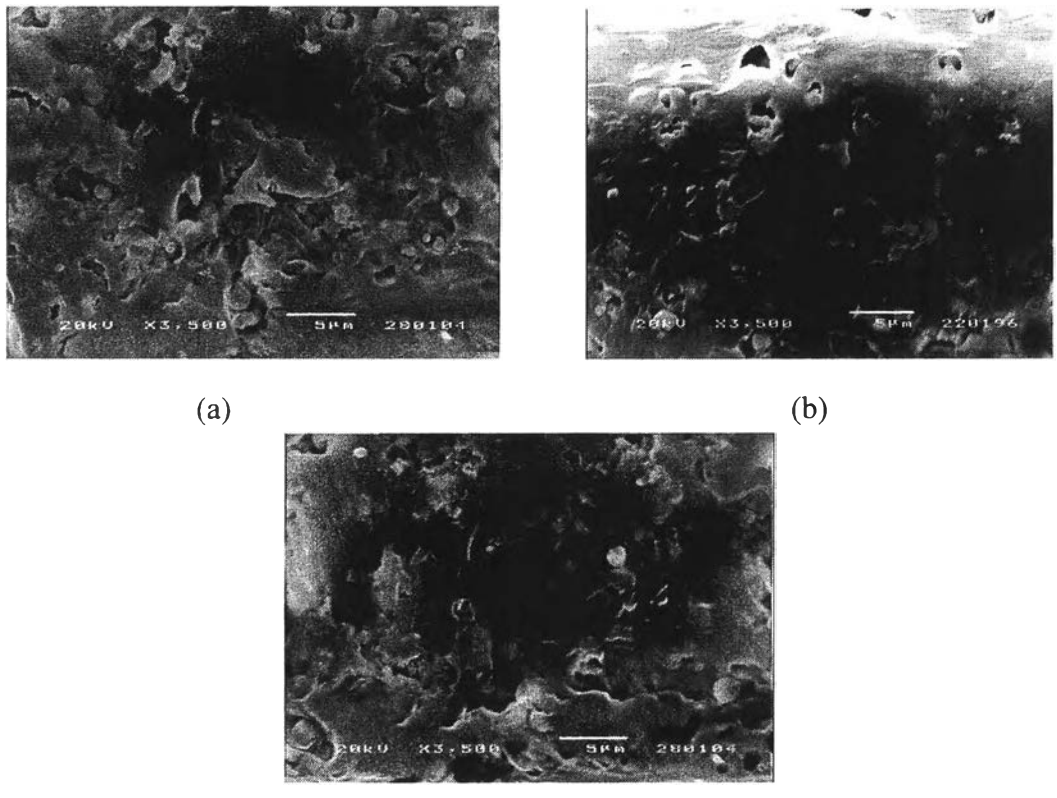

(a) (b)

(c)

Figure 4.8 SEM images showing the morphology of 20 wt% Modified zeolite-Ultem MMMs ; (a) Silicalite-Ultem MMM , (b) NaX-Ultem MMM and (c) Agx-Ultem MMM.

By comparing these three photographs with Figure 4.2, it becomes very clear that the presence of silane coupling agent improves to a large extent the internal structure of mixed matrix membrane by reducing the nonselective voids between zeolite surfaces and polymer chains. Thus, the compatibility between zeolite surfaces and polymer chains can be enhanced by such a method which provides the advantage of enabling production of a reduce-void free mixed matrix membrane.

4.3 Permeability and Selectivity for Ultem Membrane and modified Zeolite-Ultem MMMs.

The permeability measurements for Zeolite-Ultem MMMs with modified NaX, AgX and silicalite incorporated at various loadings of 10, 20 and 30 wt % were carried out in the same manner as described in Section 4.1.

4.3.1 Modified Silicalite-Ultem MMMs

The permeabilities and C_3H_6/C_3H_8 selectivity of modified Silicalite-Ultem MMMs are shown in Figure 4.9.

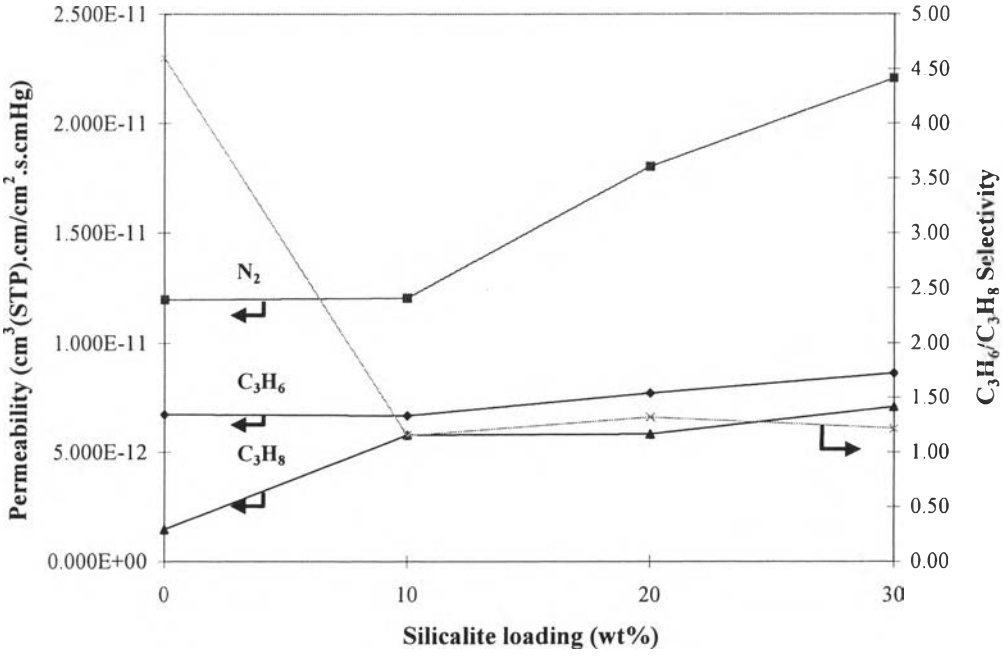

Figure 4.9 The permeabilities and C_3H_6/C_3H_8 selectivity of modified Silicalite-Ultem MMMs.

It can be cleary seen that that incorporation of Silicalite into Ultem membrane results in increasing N_2, C_3H_6 and C_3H_8 permeabilities as and increase in increasing silicalite loading. However, the C_3H_6/C_3H_8 selectivity is decreased to

around unity. Such a decrease is found to be independent of the amount of silicalite loaded in the membrane matrix.

Although there was no void formation in the matrix, the adverse results were obtained. In order to understand the effect of zeolite filling on the gas transport properties through MMMs, a facilitation ratio which is a measurement of the zeolite contribution to the permeability with respect to pure polymer was introduced (Jia *et al.* 1991). The facilitation ratio is defined as

$$F.R. = \frac{P_{z+p} - P_p}{P_p} \quad (5)$$

where P_{z+p} is the gas permeability of zeolite-polymer MMM and P_p is the gas permeability of pure polymer. The term $P_{z+p} - P_p$ is the permeability difference between zeolite-filled MMM and zeolite-free polymer membrane, which represents the permeability contributed by zeolite.

From the Equation (5), in case of pure polymer membrane it is equal to zero. If it is positive, indicating that the zeolite in the matrix can help the passage of the gas molecules. The zeolite hinders the transport of the gas molecules when the ratio is negative. However, the overall permeability through MMM is the sum of the permeability from both zeolite and polymeric phase. Facilitation ratios of gas for Modified Silicalite-Ultem MMMs are given in Figure 4.10.

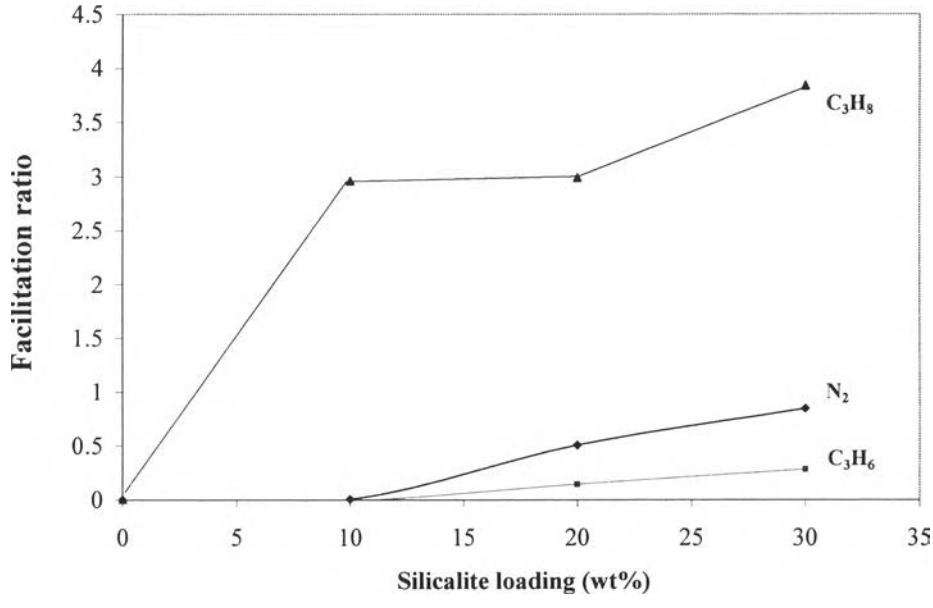

Figure 4.10 Facilitation ratio contributed by modified Silicalite to the gas permeation.

As can be seen from the figure, the facilitation ratios of gas through modified Silicalite-Ultem MMMs are positive for all gases studied, and increased with increasing Silicalite loading. Therefore, Silicalite in the matrix can help the passage of all gas molecules through the MMMs when compared to the Silicalite-free Ultem membrane. In the range of Silicalite loading studied, the facilitation ratio for C_3H_6 was the lowest among three gases studied. It is believed to be due to its highest dipole moment (N_2 = 0, C_3H_8 = 0.084 and C_3H_6 = 0.366 Debye, Chemical Properties Handbook, P.245-261) in which it is not compatible with hydrophobicity of Silicalite (Si/Al = 130). This phenomenon might be expected to occur when the size of gas molecule and the pore size of zeolite are similar to each other as observed in this case (pore opening of Silicalite = 5.3-5.6<->5.1-5.6 Å, kinetic diameter of N_2 C_3H_6 and C_3H_8 = 3.64, 4.50 and 4.30 Å, respectively). However, it would have another effect related would be considered since the differences in facilitation ratio of N_2 and C_3H_8 were observed even if their dipole moment are quite similar. The difference in dipole polarizability (the average dipole polarizability at ground state

(10^{-24} cm^3) of N_2 = 1.7403, C_3H_8 = 6.26 and C_3H_6 = 6.29) would be considered as another effect occurring while these two species flow through the pore of Silicalite. Thus, the higher dipole polarizable molecule, C_3H_8, would be easier to be polarized that results to be incompatible with hydrophobic surface of Silicalite. As a result, facilitation ratios of C_3H_8 were higher than N_2. Not only can Silicalite in the matrix preferentially facilitate C_3H_8 greater than C_3H_6 but it also results in increasing the overall C_3H_8 permeabilities to the value that is almost equal to the overall C_3H_6 permeability. This is why C_3H_6/C_3H_8 selectivity is low to almost no separation.

4.3.2 Modified NaX-Ultem MMMs

The permeabilities and C_3H_6/C_3H_8 selectivity of modified NaX-Ultem MMMs are shown in Figure 4.11.

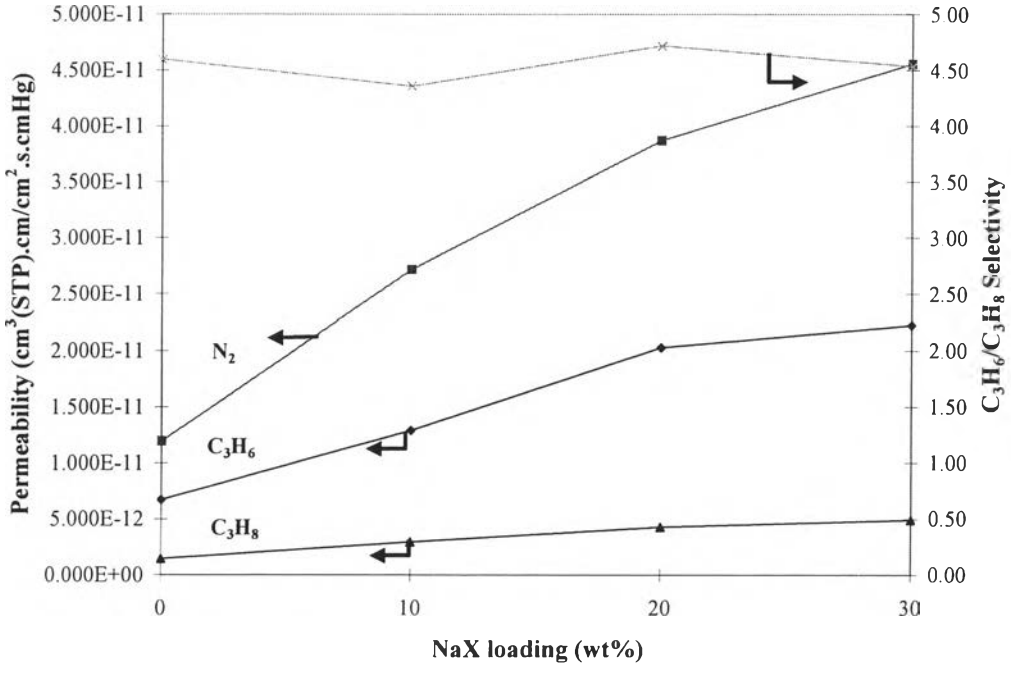

Figure 4.11 The permeabilities and C_3H_6/C_3H_8 selectivity of modified NaX-Ultem MMMs.

For the results of modified NaX-Ultem MMMs, incorporation of NaX (Si/Al = 1.2) into Ultem membrane results in increasing in the N_2, C_3H_6 and C_3H_8

permeabilities, as an increase in NaX loading. However the C_3H_6/C_3H_8 selectivity is significant changed as compared to that of Ultem membrane, and is almost independent of the amount of NaX loaded in the membrane matrix.

Facilitation ratios of gas for modified NaX-Ultem MMMs are presented in Figure 4.12.

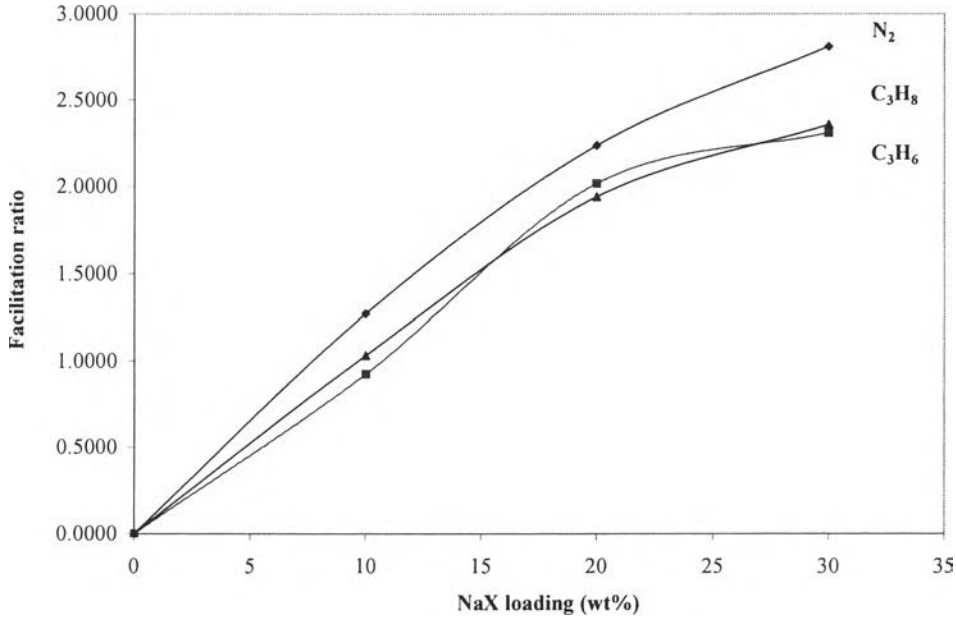

Figure 4.12 Facilitation ratio contributed by modified NaX to gas permeation.

As can be seen from Figure 4.12, the facilitation ratios of gas through modified NaX-Ultem MMMs were positive for all gases studied, and increased with increasing NaX loading. Therefore, NaX can help the passage for all gas molecules through the MMMs when compared to that of Ultem membrane. In the range of NaX loading studied, the facilitation ratio for N_2 is the highest whereas those for C_3H_6 and C_3H_8 are almost the same. The reason for that can be explained when considering the molecular size of each molecule. The molecular size of N_2 is the smallest among three gases, but almost no molecular size difference between C_3H_6 and C_3H_8. Therefore, it is believed that NaX in the matrix plays a molecular sieving role in gas separation through such MMMs. Due to the similar molecular sizes of C_3H_6 and C_3H_8 , NaX can facilitate these molecules passing through in a similar

manner. However, the C_3H_6/C_3H_8 separation took place predominantly in the polymer phase, as a results the C_3H_6/C_3H_8 selectivity seems to be unchanged.

4.3.3 Modified AgX-Ultem MMMs

The permeabilities and C_3H_6/C_3H_8 selectivity of modified AgX-Ultem MMMs are shown in Figure 4.13.

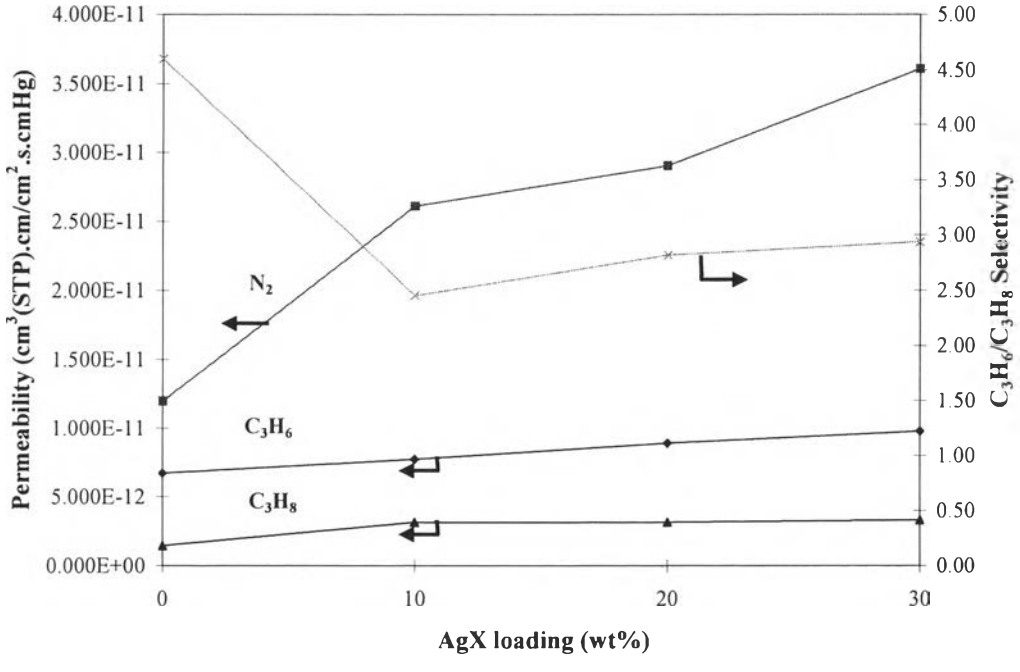

Figure 4.13 The gas permeabilities and the C_3H_6/C_3H_8 selectivity of modified AgX-Ultem MMMs.

As can be seen, incorporation of AgX (Si/Al = 1.2) into Ultem membrane exhibits increases in N_2, C_3H_6 and C_3H_8 permeabilities, as an increase in AgX loading. A decrease in C_3H_6/C_3H_8 selectivity relative to that of Ultem membrane was observed to be independent of the amount of AgX loaded in the membrane matrix.

Facilitation ratios of gas for modified AgX-Ultem MMMs are shown in Figure 4.14.

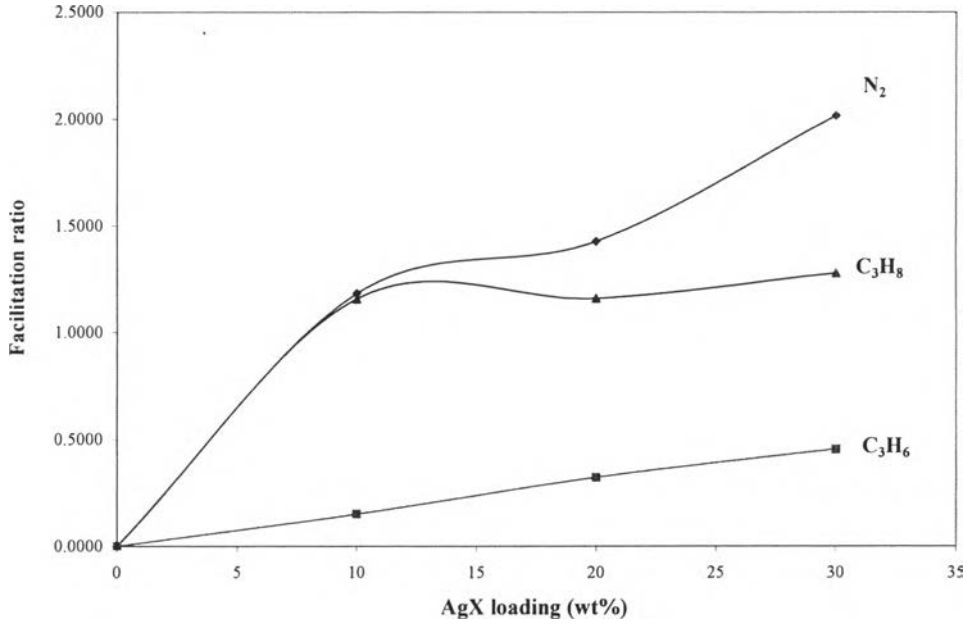

Figure 4.14 Facilitation ratio contributed by modified AgX to gas permeation.

The facilitation ratios for modified AgX-Ultem MMMs are positive for all gases studied, and increased with increasing AgX loading. This can be explained in the same reason as for Silicalite and NaX. In the range of AgX loading studied, the facilitation ratio for N_2 is the highest. Therefore, the first major role contributed by AgX for C_3H_6/C_3H_8 separation through such a MMMs was the molecular sieve effect same as Modified NaX-Ultem MMMs. Due to the smallest molecule of N_2, AgX preferentially facilitates it more than C_3H_6 and C_3H_8. The molecular size of C_3H_6 and C_3H_8 are quite similar; however, AgX can facilitate C_3H_8 greater than C_3H_6 , even if the intrinsic properties of AgX zeolite is hydrophilic and the previous study found that it is more selective to olefin over paraffin with testing equilibrium adsorption process. Therefore, there is another effect involved. Since Ag^+ can form π complexzation with olefin, it might be expected to occur in our study as well. From this interaction, AgX might not allow C_3H_6 to desorp under condition applied. Therefore, AgX can facilitate C_3H_8 greater than C_3H_6. The overall

permeability is sum of the permeability of both two phases; zeolite and polymer, so when incorporated AgX which in the matrix it prefers to facilitate C_3H_8 more than C_3H_6 into C_3H_6 selective polymer, Ultem membrane, resulted in decrease in C_3H_6/C_3H_8 selectivities compared to that of Ultem membrane.

4.4 Comparisons of Permeability and Selectivity Between Zeolite-Ultem MMMs and modified Zeolite-Ultem MMMs

The comparisons of the permeabilities and the C_3H_6/C_3H_8 selectivities through the zeolite-Ultem MMMs and modified zeolite-Ultem MMMs are graphically presented in Figures 4.15 - 4.18.

In order to solve the problem of void formation between polymer chains and zeolite particles in the membrane matrix, aminofuctional silane agent was successfully introduced to modified surface of zeolite to make them more compatible with polymer chains that can be evidenced from the results of FTIR spectroscope and SEM images. When compared the permeability and the C_3H_6/C_3H_8 selectivity results received between MMMs with and without modification of surface of zeolite, the better adhesion of zeolite-polymer chain contact accounts for decreasing in the gas permeabilities without any improvement in the C_3H_6/C_3H_8 selectivities. Therefore, no separation took place in such a voids for our MMMs. However, once no voids appear in the matrix, the explanation of the real function of zeolite that contributes to the membrane performances for separation can be clearly given.

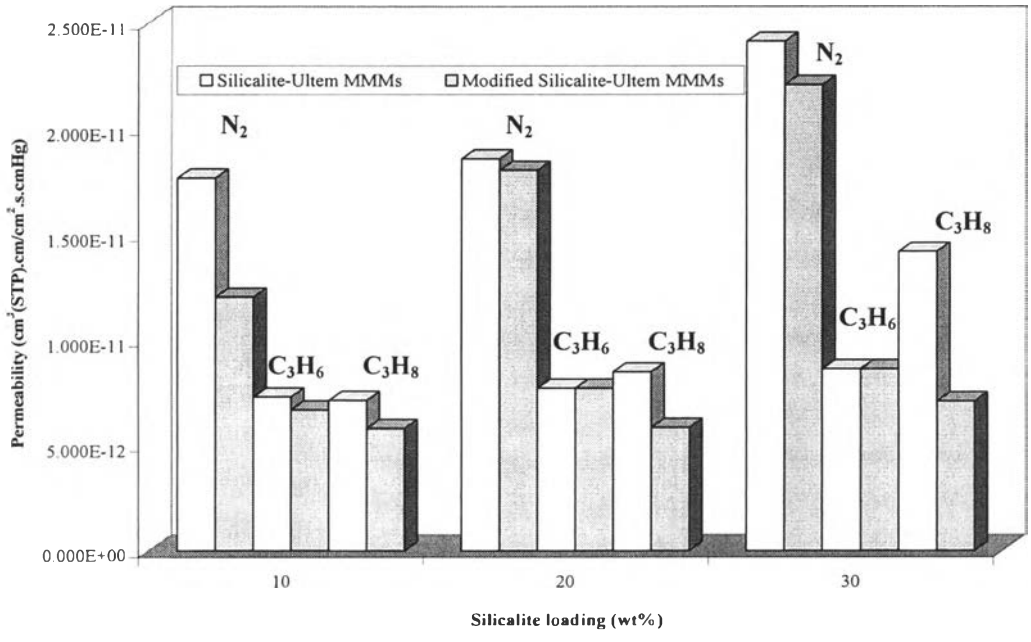

Figure 4.15 The comparison of the permeabilities through Silicalite-Ultem MMMs and modified Silicalite-Ultem MMMs.

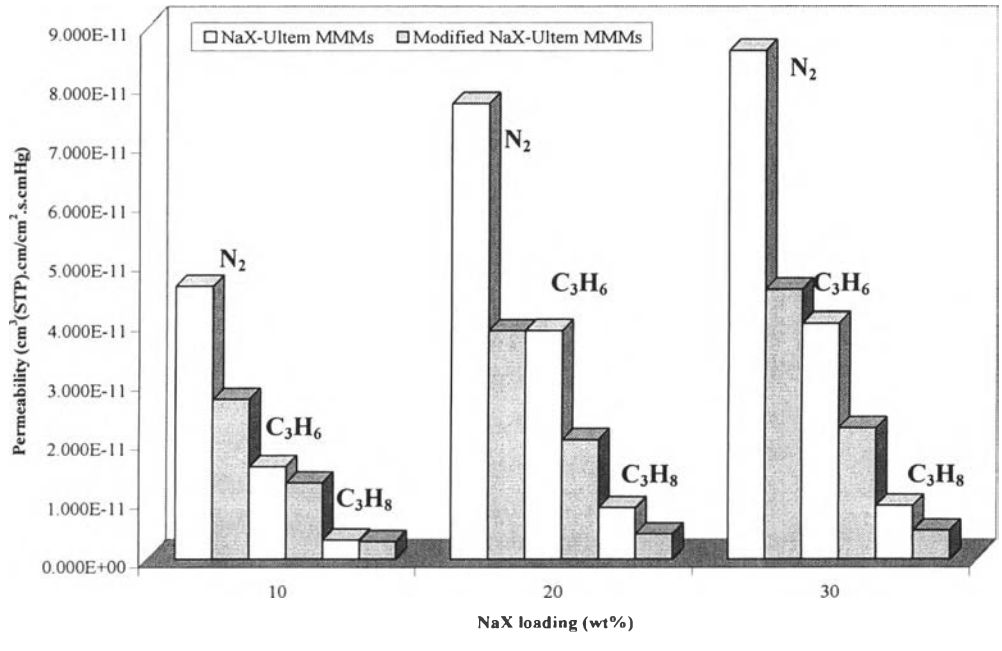

Figure 4.16 The comparison of the permeabilities through NaX-Ultem MMMs and modified NaX-Ultem MMMs.

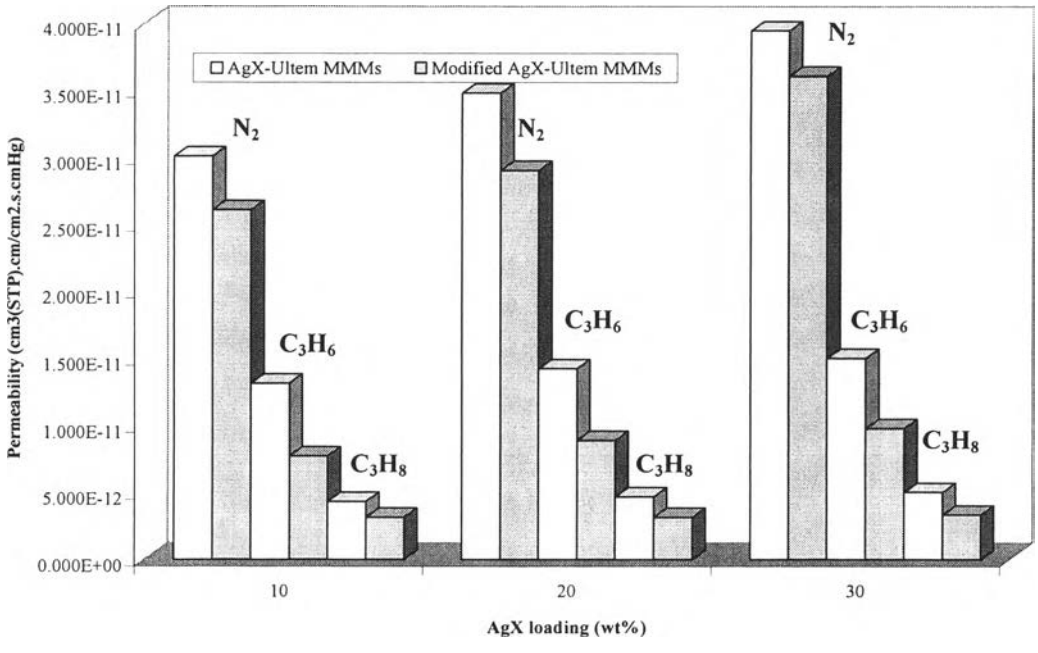

Figure 4.17 The comparison of the permeabilities through AgX-Ultem MMMs and modified AgX-Ultem MMMs.

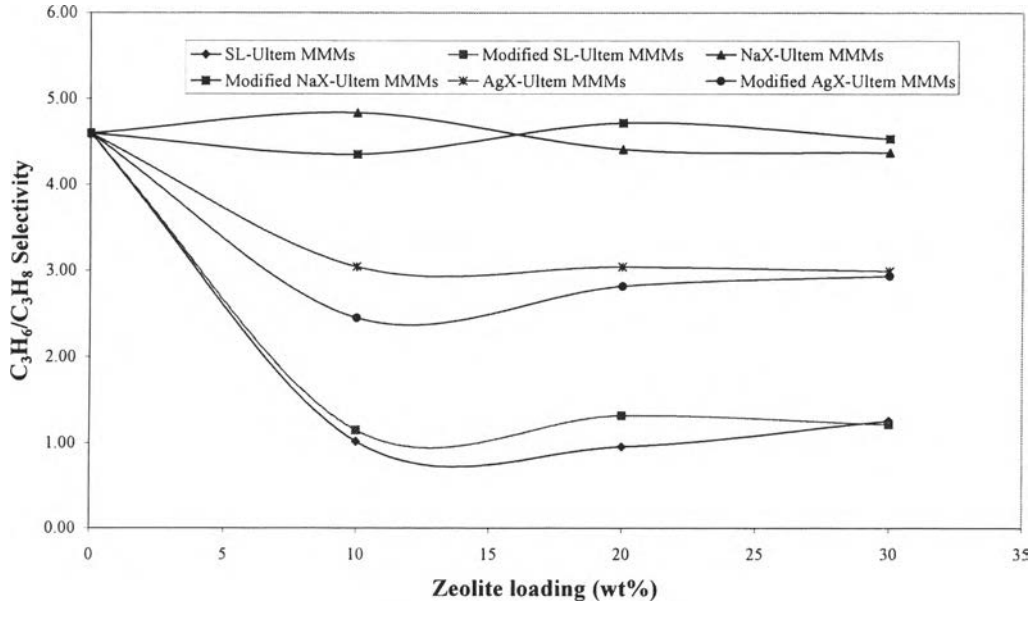

Figure 4.18 The comparison of the C_3H_6/C_3H_8 selectivity through zeolite-Ultem MMMs and modified zeolite-Ultem MMMs.